

Investigation of physicochemical properties and radiation resistance of fullerene and endohedral metallofullerene derivatives under the ionizing radiation influence

M. V. Suyasova, A. A. Borisenkova, V. A. Shilin, V. P. Sedov, D. N. Orlova

B. P. Konstantinov Petersburg Nuclear Physics Institute, NRC Kurchatov Institute,
Leningradskaya oblast, Gatchina, 1 mkr. Orlova roshcha, 188300, Russia

suyasova_mv@pnpi.nrcki.ru, borisenkova_aa@pnpi.nrcki.ru, shilin_va@pnpi.nrcki.ru,
victorsedov61@gmail.com, orlova_dn@pnpi.nrcki.ru

PACS 61.48.+c

DOI 10.17586/2220-8054-2019-10-4-447-455

The radiation resistances of fullerenes C_{60} and C_{70} , end metallofullerenes $Me@C_{2n}$ ($n = 30 - 50$), derivatives $C_{60}(OH)_{(30)}$ and $Me@C_{2n}(OH)_{30-40}$ ($Me = Sm, Eu, Gd, Tb, Ho, Fe, Co$), and complexes with biocompatible polymers – polyvinylpyrrolidone and dextrin – $Fe@C_{60}(C_6H_9NO)_n$, $Sm@C_{82}(C_6H_9NO)_n$, $Gd@C_{82}(C_6H_9NO)_n$ and $Fe@C_{60}(C_6H_{10}O_5)_n$ were studied. For the structures irradiated by protons with energies of 100 MeV and 1 GeV, radiation resistance was estimated. The comparison of the results of radiation resistance under irradiation by protons and reactor neutrons at fluencies from 10^{18} to 10^{19} cm^{-2} was carried out. It is shown, that endofullerenols are more stable under the proton and neutron irradiation than initial endofullerenes. The molecules containing Eu, Gd and Sm with large thermal neutron capture cross sections were found to be the most stable under neutron irradiation. The mechanism of rebuilding of secondary endofullerenols Eu, Sm, Gd, as well as other factors' influence on radiation resistance are discussed.

Keywords: fullerenes, endometallofullerenes, fullerenols, fullerene complexes with biopolymers, radiation resistance, proton irradiation, neutron irradiation.

Received: 12 June 2019

Revised: 29 June 2019

1. Introduction

The creation of therapeutic drugs capable of tumor-selective accumulation, currently remains an important task. The most promising in this medicine area are endometallofullerenes (EMF) with a metal atom in a carbon shell that is enclosed and protected from chemical attack of the *in vivo* environment. Furthermore, the irradiation of EMF in the ionizing radiation flow discovers the possibility of creating radiopharmaceuticals for the diagnosis and treatment of cancer.

The currently used chemotherapy methods don't always ensure selective delivery and effective concentration of therapeutic agents in the target tumor tissue. In conjunction with limited monitoring ability to outcome therapeutic procedure results it often leads to complications and also reduces the therapeutic effect. The development of specific tumors MRI contrast agents based on nanotechnology and nanomaterials would increase selectivity and sensitivity of non-invasive tumor-imaging in clinical practice in comparison with traditional imaging methods [1, 2].

Recent studies have found that surface-modified endofullerene $Fe@C_{60}$ with hydroxyl groups are more effective contrast agents than the iron oxide nanoparticles generally used in practical imaging [3–5].

Practical interest in biocompatible iron-containing fullerene-polymer complexes is caused by the possibility of their use for improving resolution in magnetic resonance imaging [5], as well as for molecular-targeted drug delivery in the human body, including for the cancer treatment [6].

However, EMF administration is complicated by the fact that these compounds are insoluble in water in their initial form, so their biomedical application may require modification, such as hydroxylation [7] or synthesis of complexes with water-soluble biocompatible polymers. Polymeric materials are attractive because of number of advantages determining their effectiveness in delivery and therapy techniques – biocompatibility, biodegradability, and interoperability. Basic and the most widely – used compounds for the polymer nanoparticle synthesis are polylactic (PLLA) and polyglycolicacids (PGA), polyethylene glycol (PEG), polycaprolactone (PCL), polyvinylpyrrolidone (PVP). Due to its good solubility in water and the tendency to complex formation, PVP has found wide application in medicine.

In addition, particles of contrast agents should easily penetrate cell membranes. Therefore, control of new potential objects sizes is extremely important for such medical purposes [8].

In this research of fullerene derivatives radiation resistance, fullerene and endometallofullerene complexes with biocompatible polymers have been synthesized. As polymers, the polysaccharide dextrin $(C_6H_{10}O_5)_n$, obtained by

thermal treatment of potato starch, and a synthetic polymer polyvinylpyrrolidone $(C_6H_9NO)_n$ with low molecular weight were chosen.

To develop new generation radiopharmaceuticals, it is also necessary to determine how the properties of water-soluble fullerene and EMF derivatives are altered under radiation exposure. For polymeric materials the effects of ionizing radiation on the physicochemical properties have been well studied [9–12]. However, radiation effect and, most of all, influence of proton irradiation on the fullerenes and EMF polymer complexes has not yet been described.

The main feature of proton irradiation is the possibility of observing a large number of nuclear reactions ((p, α) , (p, n) , (p, p) , (p, γ) , (p, d) etc.). The probability of the reactions becomes significant at such proton energy when the permeability of the Coulomb barrier becomes quite large [13, 14]. In this regard, the purpose of our work was to study the radiation resistance of the initial, functionalized by hydroxyl groups and biocompatible polymers (PVP, dextrin) fullerenes and EMF with 3d and 4f-elements under proton and neutron irradiation.

2. Experimental

Thermal evaporation of the composite electrode material, extraction of fullerenes and EMF with an impurity of empty fullerenes $Me@C_{2n} + C_{2n}$ ($Me = Sm, Eu, Gd, Tb, Ho, Fe, Co$) were carried out according to previously-described methods [12, 15–21].

For fullerene and EMF synthesis, hollow graphite rods with an outer diameter 10 mm and internal diameter 6 mm with different graphite density were used. The electrodes were produced by the Federal State Unitary Enterprise Scientific Research Institute of Electric Carbon Products (graphite density 1.35 g/cm^3) and Chelyabinsk company “Graphite Formula” (1.8 g/cm^3). To obtain EMF composite electrodes were prepared as follows. A powder mixture of metal oxide with graphite was introduced into the cavity of the graphite tube by pressing. The composite electrode was annealed at $1000 \text{ }^\circ\text{C}$ in vacuum (3 hours) to remove water and organic impurities. The metal content in the composite electrode was in the range 0.8 – 1.0 % at. Thermal vaporization of the composite electrode material was carried out at a constant current of an electric arc (120 – 130 Å) in helium atmosphere (608 mm Hg) according to the methods [18–21].

Figure 1 shows the dependences of higher fullerenes (productivity parameter P_{HF}) and endometallofullerenes (productivity parameter P_{EMF}) outputs from the helium pressure in the electric arc generator [16]. To determine P_{HF} and P_{EMF} parameters high performance liquid chromatography (HPLC) data was used. The productive parameter is an integrated value, including the yield of electric arc soot (wt.%), the content of extractable fullerenes (wt.%) and the content of higher fullerenes or EMF according to HPLC. As can be seen from the figure, there are two maxima: the first at 114 mm Hg and the second – in the range of 532 – 684 mm Hg. Therefore, further synthesis was performed at preferred helium pressure – 608 mm Hg. In such a way the values of the P_{HF} parameter were increased by 2 – 2.5 times as compared with P_{HF} at low pressure.

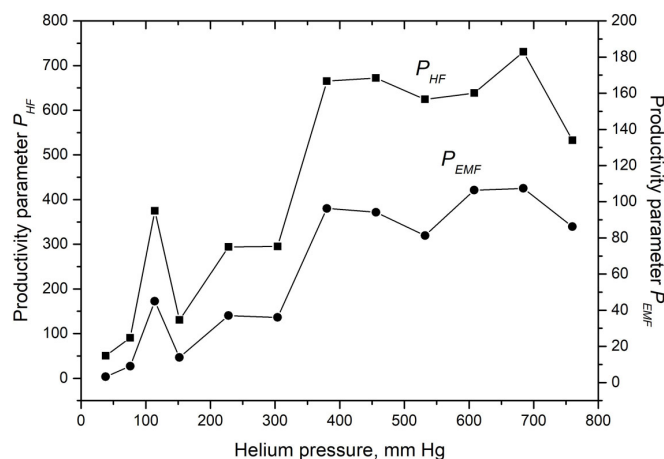


FIG. 1. The dependences of higher fullerenes productivity parameter P_{HF} and endometallofullerenes productivity parameter P_{EMF} outputs from the helium pressure [16]

Figure 2 shows the arc current influence on the productivity parameter P_{EMF} in the series of EMF synthesis with various elements of the lanthanide group: Sm (1), Gd (2), Dy (3), Eu (4), Ho (5). It can be seen that P_{EMF} is influenced by the nature of the metal atom. In the synthesis of EMF with samarium, gadolinium, and europium atoms, the current change in the studied range doesn't lead to changes in the EMF yields. At the same time, for EMF with

dysprosium, the yield decreases, but for holmium, it increases significantly. Thus, the optimum range of the electric arc current at 120 – 130 Å, in which the thermal vaporization of the composite electrode material was stable and accompanied by a high value of the EMF yield (P_{EMF}) was established.

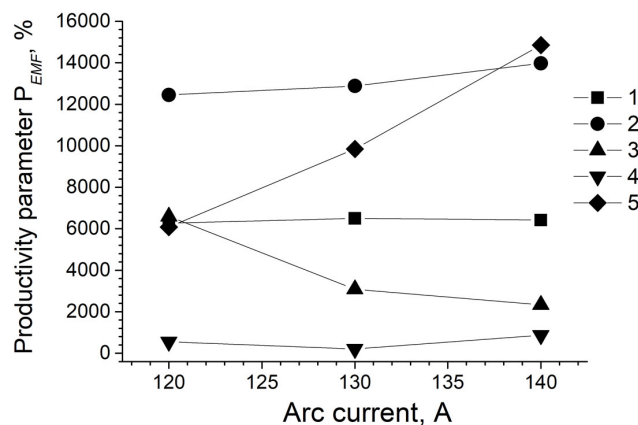


FIG. 2. The arc current influence on the productivity parameter P_{EMF} in the series of EMF synthesis with various elements of the lanthanide group: Sm (1), Gd (2), Dy (3), Eu (4), Ho (5)

For EMF derivatives identification, the IR-spectra of solid samples were obtained by multi-bounce attenuated total reflection FTIR (ATR-FTIR) in the frequency range 400 – 4400 cm^{-1} . The endofullerenol spectra illustrate absorption bands typical for fullerenols [23–25]. Characteristic bands at 1025 – 1150 cm^{-1} can be assigned $\nu\text{C-O}$ bond, reflecting the presence of oxidized units on the carbon cage. The bands at 1340 – 1387 cm^{-1} are assigned to $\delta_s\text{C-O-H}$ bond. The bands 1515 – 1625 cm^{-1} can be assigned to $\nu\text{C-C}$ and $\nu\text{C=C}$ bonds of the aromatic ring. Valence vibrations of C=O bonds in fullerenols, which formed at the ends of the broken C-C bonds of fullerene are reflected in the range 1647 – 1738 cm^{-1} . The spectra also contain characteristic absorption bands C-C of pure fullerenes C_{60} and C_{70} – 528 and 1428 cm^{-1} .

IR spectra of PVP-complexes are presented at Fig. 3. The spectra demonstrate absorption bands typical for PVP and fullerenes. The bands in the range 1020 – 1097 cm^{-1} are assigned to $\nu\text{C-O}$ bond vibrations. The characteristic bands at 1276 – 1282 cm^{-1} can be referred to the in-plane bending of the C-H bond in PVP. The 1424 cm^{-1} band of scissoring bending of the CH_2 bond in PVP overlaps the 1428 cm^{-1} absorption band of pure fullerene C-C bonds. The double bands at 1502 – 1558 cm^{-1} can be also attributed to the $\nu\text{C-C}$ and $\nu\text{C=C}$ bonds of the aromatic fullerene ring. The band of $\nu\text{C=O}$ group in the PVP lactam at 1657 cm^{-1} is overlapped the band at 1651 – 1662 cm^{-1} of $\nu\text{C=O}$ bonds in fullerenes.

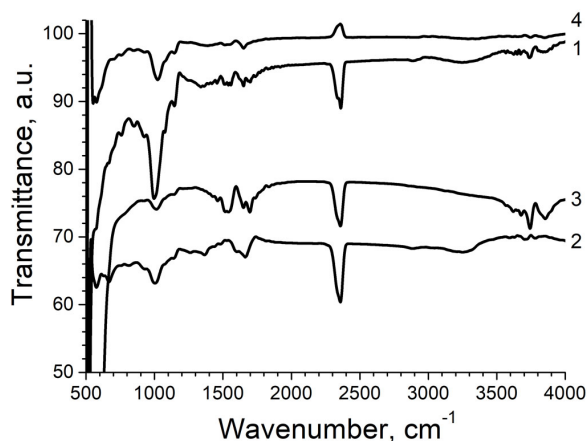


FIG. 3. IR-spectra of pure dextrin $(\text{C}_6\text{H}_{10}\text{O}_5)_n$ (1) and water-soluble dextrin complexes $\text{C}_{60}(\text{C}_6\text{H}_{10}\text{O}_5)_n$ (2), $\text{Gd@C}_{82}(\text{C}_6\text{H}_{10}\text{O}_5)_n$ (3) and $\text{Fe@C}_{60}(\text{C}_6\text{H}_{10}\text{O}_5)_n$ (4)

Similarly, during investigation of dextrin complexes IR-spectra (Fig. 4), the presence of bands that can be attributed both to dextrin and fullerenes was observed. Characteristic band of the polysaccharide molecule skeleton

vibrations shifts from 1001 cm^{-1} to $1007 - 1024\text{ cm}^{-1}$ in the complexes. Strong bands at $1360 - 1387\text{ cm}^{-1}$ in the complexes are referred to $\delta\text{O-H}$ groups in the C–O–H bond. The strong band at 1650 cm^{-1} , caused by the stretching C=O vibrations of non-ionized and ionized acids groups in dextrin, overlaps by stretching vibrations of C=O bonds in fullerenes in the range $1651 - 1662\text{ cm}^{-1}$. Broad and strong bands in the region of $3253 - 3327\text{ cm}^{-1}$ can be related to the intermolecular hydrogen bonds formation in the complexes.

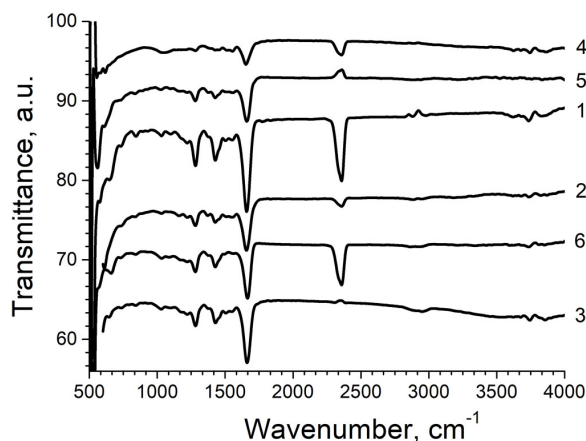


FIG. 4. IR-spectra of water-soluble polyvinylpyrrolidone $(\text{C}_6\text{H}_9\text{NO})_n$ complexes: $\text{C}_{2n}(\text{C}_6\text{H}_9\text{NO})_n$ (1), $\text{Sm}@C_{82}(\text{C}_6\text{H}_9\text{NO})_n$ (2), $\text{Ho}@C_{82}(\text{C}_6\text{H}_9\text{NO})_n$ (3), $\text{Gd}@C_{82}(\text{C}_6\text{H}_9\text{NO})_n$ (4), $\text{Eu}@C_{82}(\text{C}_6\text{H}_9\text{NO})_n$ (5), $\text{Dy}@C_{82}(\text{C}_6\text{H}_9\text{NO})_n$ (6)

Thus, by the method of IR-spectroscopy it has been able to characterize the obtained compounds and confirm the presence of fullerenes in the synthesized water-soluble complexes.

Earlier studies of the fullerene derivatives radiation resistance under neutron irradiation in the WWR-M reactor zone (NRC “Kurchatov Institute” – PNPI, Gatchina) showed that significant radiation damage and insoluble carbon aggregate formation were observed at fluences exceeding 10^{16} cm^{-2} . In this study, we investigated radiation resistance under proton irradiation on the samples of fullerenes C_{60} , C_{70} , fullerenols $\text{C}_{60}(\text{OH})_{30}$, $\text{Fe}@C_{60}(\text{OH})_{30}$ and $\text{Me}@C_{82}(\text{OH})_{38-40}$ ($\text{Me} = \text{Sm}, \text{Eu}, \text{Gd}, \text{Tb}, \text{Ho}$) and complexes $\text{Sm}@C_{82}(\text{C}_6\text{H}_9\text{NO})_n$, $\text{Gd}@C_{82}(\text{C}_6\text{H}_9\text{NO})_n$, $\text{Fe}@C_{60}(\text{C}_6\text{H}_9\text{NO})_n$, $\text{Fe}@C_{60}(\text{C}_6\text{H}_{10}\text{O}_5)_n$. The samples were irradiated at the Synchrocyclotron SC-1000 (NRC “Kurchatov Institute” – PNPI, Gatchina) by protons with energies of 100 MeV and 1 GeV (current value was varied from ~ 0.03 to $1\ \mu\text{A}$) for a time from 20 to 72 hours. After irradiation, the samples were kept for two months for the decay of short-lived radionuclides.

The γ -spectra of all irradiated samples were recorded using a semiconductor spectrometer with an ultrapure germanium detector (EG&G ORTEC Gamma-X HPGe, detector efficiency at 1 MeV energy – 5 %, resolution – 0.57 keV for 122.06 keV line of ^{57}Co). Unfortunately, it was not possible to identify all γ -lines of reactions (p, x). Therefore, for samples of endofullerenols and EMF complexes, areas of the most intense γ -lines for soluble and insoluble parts were measured. The irradiated samples radiation resistance (S , %) was estimated by the formula:

$$S(\Phi) = \frac{I_{\text{soluble}}}{I_{\text{soluble}} + I_{\text{insoluble}}} \cdot 100\%.$$

The radiation resistance (S , %) of samples C_{60} , C_{70} , $\text{C}_{60}(\text{OH})_{30}$ was determined as the ratio of the weight of the soluble part to the total weight. It should be noted, that a small amount of impurity elements could present in the irradiated samples. The neutron capture cross section of some of them can be very large. For example, the thermal neutron capture cross section in a natural mixture for Eu isotopes is 4565 barn, for Gd is 48,890 barn and for Sm is 5670 barn [26]. Such impurities were easily identified in the samples irradiated by the neutron, and in some cases by proton irradiation.

3. Results and discussion

Tables 1 and 2 present the radiation resistance of fullerenes C_{60} , C_{70} , EMF $\text{Me}@C_{2n}$ ($n = 30 - 50$), hydroxylated derivatives $\text{C}_{60}(\text{OH})_{30}$ and $\text{Me}@C_{2n}(\text{OH})_{30-40}$ ($\text{Me} = \text{Sm}, \text{Eu}, \text{Gd}, \text{Tb}, \text{Ho}, \text{Fe}, \text{Co}$), as well as complexes $\text{Fe}@C_{60}(\text{C}_6\text{H}_9\text{NO})_n$, $\text{Sm}@C_{82}(\text{C}_6\text{H}_9\text{NO})_n$, $\text{Gd}@C_{82}(\text{C}_6\text{H}_9\text{NO})_n$ and $\text{Fe}@C_{60}(\text{C}_6\text{H}_{10}\text{O}_5)_n$ under proton irradiation. The capture cross sections for main reactions proceeding at target irradiation by protons was estimated using the semi-empirical method [27] (Table 1).

TABLE 1. Radiation resistance of samples under irradiation by protons of 1 GeV

Formula	Content of $C_{2n}(OH)_{38}$, wt %	Atomic radius, pm [28]	Proton capture cross section σ , barn [26]	Radiation resistance, %
C_{60}	—	—	—	56±4
C_{70}	—	—	—	21±3
$C_{60}(OH)_{30}$	—	—	—	99±1
$Fe@C_{60}(OH)_{30}$	2.4 %	124	0.717	71±1
$Sm@C_{82}(OH)_{38-40}$	3.4 %	181	1.371	41±3
$Eu@C_{82}(OH)_{38-40}$	1.0 %	199	1.378	55±3
$Gd@C_{82}(OH)_{38-40}$	40 %	179	1.414	46±2
$Tb@C_{82}(OH)_{38-40}$	18 %	177	1.420	57±2
$Ho@C_{82}(OH)_{38-40}$	10 %	179	1.456	52±3
$Gd@C_{82}(C_6H_9NO)_n$	—	179	1.414	34±2
$Fe@C_{60}(C_6H_9NO)_n$	—	124	0.717	51±2
$Fe@C_{60}(C_6H_{10}O_5)_n$	—	124	0.717	36±1

TABLE 2. Comparison of radiation resistance for the samples irradiated by 100 MeV and 1 GeV protons

Formula	Radiation resistance, %	
	Proton energy	
	100 MeV	1 GeV
$Fe@C_{60}(OH)_{30}$	44.7±1.0	32±3
$Gd@C_{82}(OH)_{38-40}$	74±4	29±2
$Sm@C_{82}(OH)_{38-40}$	50±2	31±2
$Tb@C_{82}(OH)_{38-40}$	70±2	57±2
$Sm@C_{82}(C_6H_9NO)_n$	39.4±1.5	26±4

As can be seen from Table 1, the cross sections for EMF, including elements Sm, Gd, Eu, during proton irradiation are in the range 1.3 – 1.5 barn. The values of radiation resistance for EMF Sm, Gd, Eu are also varied slightly – 41, 46 and 55 %, respectively. Comparing the radiation resistance values obtained for hydroxylated and polymeric EMF derivatives, it should be noted that the complexes resistance is almost 20 %, and in some cases 30 % less: $Gd@C_{82}(OH)_{38-40}$ (46 %) and $Gd@C_{82}(C_6H_9NO)_n$ (34 %); $Fe@C_{60}(OH)_{30}$ (71 %), $Fe@C_{60}(C_6H_9NO)_n$ (51 %) and $Fe@C_{60}(C_6H_{10}O_5)_n$ (36 %). Probably, the nature of bond formation between polymer and EMF molecules may influence on such difference. It is known, that in the case of a complex with polyvinylpyrrolidone, donor-acceptor interaction is realized, and in the case of a complex with dextrin, a dipole-dipole interaction does [8]. Such complexes turn out to be less resistant to proton irradiation than chemically modified fullerenols with OH-groups. In addition, polymer amorphization at large fluencies can also lead to a decrease their solubility and resistance [29].

Table 2 presents radiation resistance comparison for the samples irradiated by 100 MeV and 1 GeV protons. It has been found that for a series of 1 GeV proton irradiation, the values of radiation resistance are significantly lower than for 100 MeV ones. High-energy protons lead to more damage in the EMF derivatives, which adversely affects the solubility and, as a result, the resistance values.

To compare with the proton irradiation results, the data for neutron irradiation fullerene derivative by fluence $\Phi = 2 \times 10^{18} \text{ cm}^{-2}$, at which sample differences appear clearly are shown in the Table 3. As mentioned above, in addition to compounds with 4f-metals, we studied fullerenols with cobalt, obtained for the first time in the synthesis of a new EMFs with paramagnetic 3d-metals [17].

TABLE 3. Radiation resistance of endometallofullerenols under neutron irradiation by fluence $\Phi = 2 \times 10^{18} \text{ cm}^{-2}$ [30]

Symbol	Formula	Content of $\text{C}_{2n}(\text{OH})_{38}$, wt %	Atomic radius, pm	Recoil energy, eV	Neutron capture cross section σ_{th} , barn	Radiation resistance, %
Fe	$\text{Fe}@C_{60}(\text{OH})_{30}$	24 %	124	393.3	2.56	47.0 ± 0.5
Sm	$\text{Sm}@C_{82}(\text{OH})_{38-40}$	3.4 %	181	260.3	5670	80.1 ± 0.3
Eu	$\text{Eu}@C_{82}(\text{OH})_{38-40}$	1.0 %	202	256.1	4565	90.5 ± 0.3
Gd	$\text{Gd}@C_{82}(\text{OH})_{38-40}$	40 %	179	136.4	48890	94.1 ± 0.3
Tb	$\text{Tb}@C_{82}(\text{OH})_{38-40}$	19 %	177	136.1	23.4	59.3 ± 0.7
Ho	$\text{Ho}@C_{82}(\text{OH})_{38-40}$	10 %	176	125.9	64.7	65.6 ± 0.5
Co	$\text{Co}@C_{60}(\text{OH})_{38}$	12 %	125	501.5	37.2	48.5 ± 1

The radiation resistance dependence on the accumulated fluence (F) for neutron irradiation of EMF with europium, samarium, thulium, holmium and their water-soluble derivatives are shown at Fig. 5. As a comparison sample, irradiated empty fullerenols $\text{C}_{60}(\text{OH})_{30}$ were used. It has been found that for all fullerenols with rare earth elements, the resistance rate is almost an order of magnitude higher than for initial EMFs. The increased radiation resistance of fullerenols $\text{Me}@C_{2n}(\text{OH})_{30-40}$ in compare with $\text{Me}@C_{2n}$ ($\text{Me} = \text{Sm}, \text{Eu}, \text{Ho}, \text{Co}$) may be related to EMF becomes more stable and their chemical reactivity decreases with increasing a number of hydroxyls [7]. In addition, resistance depends not only on the number of hydroxyl groups, but also on their distribution on the fullerene shell.

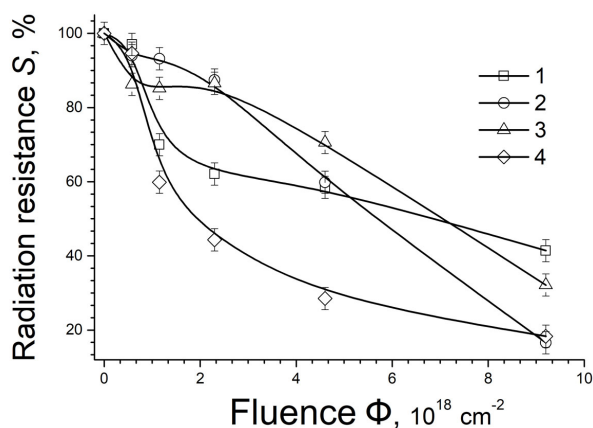


FIG. 5. Dependence of the radiation resistance (S) from fluence (Φ) for irradiated by thermal and fast neutrons fullerenols $\text{C}_{60}(\text{OH})_{30}$ (1) and endofullerenols $\text{Eu}@C_{82}(\text{OH})_{38-40}$ (2) $\text{Sm}@C_{82}(\text{OH})_{38-40}$ (3), $\text{Tm}@C_{82}(\text{OH})_{38-40}$ (4)

As shown from the Table 3, it should pay attention to the anomalously high radiation resistance near to 80 % of EMF with samarium, gadolinium and europium, whereas for other EMFs it is about 20 %. Probably, it is due to the electronic properties features of Sm@C_{2n} and Gd@C_{2n} molecules [31, 32].

It is known that $\text{Me}^{3+}@\text{C}_{2n}^{3-}$ molecules are more stable than $\text{Me}^{2+}@\text{C}_{2n}^{2-}$. However, captured by a carbon molecule samarium (III) becomes a $\text{Sm}^{2+}@\text{C}_{76}^{2-}$. Also, among the $\text{Me}^{2+}@\text{C}_{2n}^{2-}$ molecules, EMF with samarium is the most stable and resistant to external influences, including neutron irradiation. In addition, the EMF with samarium has an important feature – it does not obey the isolated pentagons rule [30]. It is not excluded that this feature may affect the radiation resistance of unique molecule $\text{Sm}^{2+}@\text{C}_{76}^{2-}$.

The endohedral metallofullerene Gd@C_{82} is also distinguished by high radiation resistance, which may be associated with the anomalouselectronic structure of the molecule [16, 17]. In previous studies [34–36], it was established that Gd^{+3} ion in the carbon cage is located near the hexagonal ring. So EMF molecule Gd@C_{82} acquires the same properties as La@C_{82} , Sc@C_{82} .

In general, EMF radiation resistance depends on a number of factors: the metal ion radius, shape and size symmetry of EMF molecules, carbon cage electronic structure and incapsulated atom localization, presence of C_{2n} empty fullerenes (see Table 1), and the nonradiative de-excitation of EMF molecules [34, 35]. But none of them explains the high radiation resistance of EMF molecules with Sm, Gd, Eu irradiated by neutrons.

Remarkable that anomalously high resistance ($\sim 80 - 90\%$) in the stream of fast and slow neutrons is demonstrated by molecules (Table 2) containing Sm, Eu and Gd elements with large thermal neutrons capture cross sections (5670, 4600, 48,890 barn, respectively). These cross sections are several orders of magnitude larger than cross sections, for example, for Ho, Tb, and Co (64.7, 8.97, 37.2 barn, respectively) [26]. We assumed, that the causes of the anomalously high radiation resistance of EMF with Sm, Eu and Gd could be large cross sections and the secondary processes of EMF reproduction during continued exposure on the samples by thermal neutrons [30].

In this connection, it is of great interest to compare the results of proton and neutron irradiation. As can be seen from Table 1, the cross sections for targets irradiated by protons, including elements Sm, Gd, Eu, are in the range from 1.3 to 1.5 barn, just as for Ho and Tb. The radiation resistance values for EMF Sm, Gd, Eu and Ho, Tb are also not significantly different (41, 46, 55 % and 52, 57, respectively). For samples containing Sm, Eu, Gd, the calculated values of the nuclei recoil energy is approximately 260 eV. Such values are sufficient for the atoms to leave the carbon cage and can penetrate into the surrounding neighboring molecules. Therefore, it can be expected accelerated dissociation of the initial endohedral complexes and, at the same time, new endofullerenol reproduction.

It is interesting to note that the properties of EMF molecules, for example with gadolinium and lanthanum, are the same. Also, the symmetry of the C_{82} cage of Gd@C_{82} is the same as La@C_{82} . With all the similarity of gadolinium and lanthanum endofullerenes properties, there is a significant difference – the thermal neutron capture cross section of gadolinium (48,890 barn, unlike lanthanum 8.97 barn) and, as a result, the radiation resistance of gadolinium EMF is much greater than that of lanthanum EMF (80 and 25 %, respectively).

Consequently, it can be argued, that high radiation resistance of Sm, Eu, Gd EMFs in comparison with other EMFs, is associated with a large values of thermal neutrons capture cross sections and new EMFs regeneration during continued exposure on the samples by thermal neutrons. And the influence of electronic structure features of EMF molecules with Sm, Eu, Gd is small or completely absent.

4. Conclusion

Fullerenes, endometallofullerenes Me@C_{2n} ($n = 30 - 50$) and their hydroxylated water soluble derivatives as $\text{C}_{60}(\text{OH})_{30}$, $\text{Me@C}_{2n}(\text{OH})_{30-40}$ ($\text{Me} = \text{Sm, Eu, Gd, Tb, Ho, Fe, Co}$), and also complexes with biocompatible polymers – polyvinylpyrrolidone and dextrin – $\text{Fe@C}_{60}(\text{C}_6\text{H}_9\text{NO})_n$, $\text{Sm@C}_{82}(\text{C}_6\text{H}_9\text{NO})_n$, $\text{Gd@C}_{82}(\text{C}_6\text{H}_9\text{NO})_n$ and $\text{Fe@C}_{60}(\text{C}_6\text{H}_{10}\text{O}_5)_n$ have been synthesized and characterized. By the method of IR-spectroscopy, the characteristic bands of water-soluble derivatives have been established and the presence of fullerenes in the new synthesized water-soluble complexes has been confirmed.

In the series of irradiation by neutrons and protons, the radiation resistance evaluation was carried out for fullerenes, EMF, derivatives and complexes: C_{60} , C_{70} , $\text{C}_{60}(\text{OH})_{30}$, $\text{Fe@C}_{60}(\text{OH})_{30}$ and $\text{Me@C}_{82}(\text{OH})_{38-40}$ ($\text{Me} = \text{Eu, H, Sm, Gd, Tb, C}$), $\text{Fe@C}_{60}(\text{C}_6\text{H}_9\text{NO})_n$, $\text{Sm@C}_{82}(\text{C}_6\text{H}_9\text{NO})_n$, $\text{Gd@C}_{2n}(\text{C}_6\text{H}_9\text{NO})_n$, $\text{Fe@C}_{60}(\text{C}_6\text{H}_{10}\text{O}_5)_n$. The values of their radiation resistance under proton irradiation has been determined for the first time. It is shown, that irradiated by protons and neutrons $\text{Me@C}_{82}(\text{OH})_{38-40}$ are an order of magnitude more stable than initial EMFs. This is probably due to hydroxyl groups that insulate carbon shells and prevent fullerenes carbon-carbon bonding between fullerene molecules.

The irradiation result comparison of Sm, Eu, and Gd EMF-ols with high reactor neutrons capture cross sections (5670, 4600, 48,890 barns, respectively) by neutrons and protons was made. The reaction cross sections for the indicated isotopes of Sm (1.371 barn), Eu (1.378 barn) and Gd (1.414 barn) under proton irradiation are comparable

to Ho (1.456 barn) and Tb (1.420 barn) isotopes. The radiation resistance of fullereneols with Sm, Eu and Gd (41, 55, 46 %) also differs insignificantly from Ho, Tb and Co (52, 57 %) fullereneols. Consequently, it can unequivocally be argued, that high radiation resistance of Sm@C₈₂(OH)_{38–40} and Gd@C₈₂(OH)_{38–40} under neutron irradiation is associated with a large values of thermal neutrons capture cross sections and new EMFs regeneration. In such a way, the influence of electronic structure features of EMF molecules with samarium and gadolinium is small or completely absent.

It can be concluded, at samples variation fundamental differences in the obtained product characteristics haven't been found. It makes it possible using general irradiation conditions for a number of carbon and metal-carbon structures, both initial and water-soluble. It has been established, despite the large proton energy 1 GeV after prolonged irradiation up to 72 hours, up to 50 % EMF molecules remain intact and suitable for the preparation of new radiopharmaceuticals based on fullerenes, EMP and their derivatives for biomedicine.

References

- [1] Piotrovsky L.B., Kiselev O.I. *Fullerenes in biology*, Rostock, SPb, 2006, 336 p.
- [2] Anokhin Yu.N. Nanotechnologies and nanomaterials for the visualization and therapy of malignant tumors. *The success of modern science*, 2014, **5** (2), P. 14–25.
- [3] Lebedev V.T., Kulvelis Yu.V., et al. Biocompatible water-soluble endometallofullerenes: peculiarities of self-assembly in aqueous solutions and ordering under an applied magnetic field. *Nanosystems: physics, chemistry, mathematics*, 2016, **7** (1), P. 22–29.
- [4] Lebedev V.T., Szhogina A.A., Bairamukov V.Yu. Small angle neutron and X-ray studies of carbon structures with metal atoms. *J. Phys.: Conf. Series*, 2017, **848**, 012005.
- [5] Ferrucci J.T., Stark D.D. Iron oxide-enhanced MR imaging of the liver and spleen: Review of the first 5 years. *Am. J. Roentgenol.*, 1990, **155**, P. 943–950.
- [6] Kalambur V.S., Longmire E.K. Cellular level loading and heating of superparamagnetic iron oxide nanoparticles. *Langmuir*, 2007, **23**, P. 12329–12336.
- [7] Djordjevic A., et al. Review of synthesis and antioxidant potential of fullereneol nanoparticles. *Journal of Nanomaterials*, 2015, **16** (1), 280.
- [8] Yevlampieva N.P., et al. Polymer-endofullerene Fe@C₆₀ complexes for biomedical applications. *Vestnik SPSU. Physics and chemistry*, 2018, **5** (63).
- [9] Aryutkin K.N., et al. Investigation of the structural features of titanium-polymer composite materials irradiated by protons and electrons. *Proceedings of higher educational institutions*, 2011, **1/2**, P. 44–50.
- [10] Pavlenko V.I., et al. The phenomena of electrification dielectric polymer composite under the action of a stream of high-energy protons. *Proceedings of the Samara Scientific Center of the Russian Academy of Sciences*, 2010, **12** (4–3), P. 677–681.
- [11] Borisov A.M., et al. Modeling the impact of space factors on composite ceramic layers on aluminum alloys. *Physics and chemistry of materials processing*, 2012, **5**, P. 27–30.
- [12] Lebedev V.T., et al. Investigation of radiation resistance of fullerenes under irradiation with fast neutrons. *Physics of the Solid State*, 2014, **56** (1), P. 178–182.
- [13] Harutyunyan G.S. Acceleration methods for obtaining technetium 99M – technology of preparation and processing of the target and beam control, Diss. for the degree of Ph.D., Yerevan, 2016.
- [14] Khmelev A.V., Bakay P.S. Features of ¹²⁴I cyclotron production for PET diagnostics during proton irradiation of ¹²⁴TeO film. *Medical Physics*, 2013, **4**, P. 52–59.
- [15] Szhogina A.A., Shilin V.A., Sedov V.P., Lebedev V.T. Radiation resistance of endohedral metallofullerenols under neutron irradiation. *Crystallogr. Reports*, 2016, **61** (4), P. 666–669.
- [16] Shilin V.A., Lebedev V.T., Sedov V.P., Szhogina A.A. Synthesis and radiation resistance of fullerenes and fullerene derivatives. *Crystallogr. Reports*, 2016, **61** (4), P. 670–674.
- [17] Shilin V.A., et al. Fullerenes and Fullereneols survival under irradiation. *Nanosystems: physics, chemistry, mathematics*, 2016, **7** (1), P. 146–152.
- [18] Method of producing fullerene C₇₀, Patent.2455230C2 Russia: MPK B01D11/02, B01D15/08, B01D9/00, B82B3/00, B82Y40/00, C01B31/02, Sedov V.P., Kolesnik S.G., N 2010134077/05A, Issue N 19.
- [19] Method of producing highly water-soluble fullereneols, Patent.2558121C1 Russia: MPK B82B3/00, B82Y40/00, C01B31/02, C07C29/03, Sedov V.P., Szhogina A.A., N 2014113248/05A, Issue N 21.
- [20] Method of producing 3d-metal endofullerene, Patent. 2664133C1 Russia: MPK C01B 32/156, B82B 3/00, B82Y 40/00, Sedov V.P., Szhogina A.A., Suaysova M. V., Lebedev V.T., N 2017108883A, Issue N 23.
- [21] Method for producing water-soluble hydroxylated derivatives of endometallofullerenes of lanthanides, Patent. 2659972C1 Russia: MPK C01B 32/156, B82B 3/00, B82Y 40/00, Sedov V.P. Szhogina A.A., Suaysova M.V., Shilin V.A., Lebedev V.T., No. 2016151106A, Issue No. 19.
- [22] Shilin V.A., et al. Investigation of the neutron activation of endohedral rare earth metallofullerenes. *Crystallography Reports*, 2011, **56** (7), P. 1192–1196.
- [23] Kokubo K., et al. Facile synthesis of highly water-soluble fullerenes more than half-covered by hydroxyl groups. *ACS nano*, 2008, **2** (2), P. 327–333.
- [24] Husebo L.O., Sitharaman B., et al. Fullereneols revisited as stable radical anions. *Journal of the American Chemical Society*, 2004, **126** (38), P. 12055–12064.
- [25] Chiang L.Y., Upasani R.B., Swirczewski J.W., Soled S. Evidence of hemiketals incorporated in the structure of fullerols derived from aqueous acid chemistry. *Journal of the American Chemical Society*, 1993, **115** (13), P. 5453–5457.
- [26] Belanova T.S., Ignatyuk A.V., Pashchenko A.B., Plyaskin V.I. Radiative Neutron. Capture – Handbook. Energoatomizdat, Moscow, 1986, 248 p. (in Russian)
- [27] Schmitt C., Schmidt K.-H., Keli'c-Heil A. SPACS: A semi-empirical parameterization for isotopic spallation cross sections. *Physical Review*, 2014, **90** (6), 064605.

- [28] Mishenina L.M., Shelkovnikov V.V. Reference materials in chemistry, educational and methodical manual. 2007, URL: <https://ido.tsu.ru/schools/chem/data/files/spravochnik.pdf>.
- [29] Malik B., Panigrahi, S. Effect of amorphization cross-section of polymer due to MeV-proton irradiation. *Applied Physics*, 2012, **1**, P. 20–25.
- [30] Dubovskii I.M., et al. Study of the Radiation Resistance of Endohedral Fullerenes of Rare-Earth Elements and Their Water-Soluble Derivatives. *Crystallography Reports*, 2018, **63** (1), P. 132–138.
- [31] Dunsch L., Krause M., Noack J., Georgi P. Endohedral nitride cluster fullerenes: Formation and spectroscopic analysis of $L3xMxN@C2n$ ($0x3$; $N = 39, 40$). *Journal of Physics and Chemistry of Solids*, 2004, **65** (2–3), P. 309–315.
- [32] Kobayashi K., Nagase S. Structures and electronic states of $M@C82$ ($M = Sc, Y, La$ and lanthanides). *Chemical physics letters*, 1998, **282** (3–4), P. 325–329.
- [33] Hao Y., et al. $Sm@C2v(19138)-C76$: A non-IPR cage stabilized by a divalent metal ion. *Inorganic chemistry*, 2015, **54** (9), P. 4243–4248.
- [34] Mizorogi N., Nagase S. Do $Eu@C82$ and $Gd@C82$ have an anomalous endohedral structure?. *Chemical physics letters*, 2006, **431** (1–3), P. 110–112.
- [35] Liu L., et al. The structural determination of endohedral metallofullerene $Gd@C82$ by XANES. *Chemical Communications*, 2008, **4**, P. 474–476.
- [36] Sebetci A., Richter M. $Gd@C82$: origin of the antiferromagnetic coupling between endohedral Gd and the free spin on the carbon cage. *The Journal of Physical Chemistry C*, 2009, **114** (1), P. 15–19.
- [37] Grushko Y.S., et al. Radioactive metallofullerenes: Hot atom chemistry aspects. *Fullerenes, Nanotubes, and Carbon Nanostructures*, 2006, **14** (2–3), P. 249–259.
- [38] Averbukh V., Cederbaum L.S. Interatomic electronic decay in endohedral fullerenes. *Physical review letters*, 2006, **96** (5), 053401.